# The Influence of Sea-Surface Temperature on Surface Wind in the Eastern Equatorial Pacific: Weekly to Monthly Variability*

S. P. HAYES AND M. J. MCPHADEN

*Pacific Marine Environmental Laboratory, National Oceanic and Atmospheric Administration, Seattle, Washington*

J. M. WALLACE

*Department of Atmospheric Sciences, University of Washington, Seattle, Washington*

(Manuscript received 27 February 1989, in final form 3 August 1989)

ABSTRACT

Temporal correlations between near-equatorial surface wind and sea-surface temperatures (SST) at 110°W in the eastern Pacific Ocean are investigated using data from an array of moored sensors between 5°N and 5°S. The signature of tropical instability waves with periods of 20–30 days is apparent in time series of SST and both the meridional and zonal wind components. Results indicate the existence of a band of pronounced horizontal divergence in the surface wind field associated with the large meridional SST gradient (equatorial front) normally located just north of the equator. Perturbations of the equatorial front by the instability waves induce fluctuations in the overlying winds. Evidence of the air–sea coupling is stronger in time series of the meridional gradients of wind and SST than between time series of the variables themselves. The meridional differencing serves as a high-pass filter in the space domain, which removes planetary-scale wind fluctuations that are unrelated to the local SST perturbations. The wind fluctuations observed in association with tropical instability waves are on the order of 1–2 m $s^{-1}$.

These results indicate that SST variability on weekly to monthly time scales forces perturbations in the surface wind field. It is suggested that the principal coupling mechanism in this region is the modification of the atmospheric boundary layer stratification. Over the equatorial cold SST tongue the vertical wind shear within the lowest 100 m of the atmosphere is strong and the surface winds are conspicuously weak. As the air flows northward across the equatorial front the boundary layer becomes destabilized, momentum is mixed downward, and the surface winds increase.

## 1. Introduction

Climatological mean and interannual variability of the sea-surface temperature (SST) and surface wind fields in the eastern equatorial Pacific are discussed in Wallace et al. (1989). Prominent features of the SST distribution are the equatorial cold tongue, which is centered slightly south, and the equatorial front, which (west of the Galápagos Islands) is located slightly north of the equator. These features are modulated seasonally and interannually. During the equatorial warm season (March through June) surface temperatures colder than 25°C are confined to the upwelling region near the South American coast (Fig. 1); the equatorial front is weak or nonexistent. During the cold season (July through November) the equatorial cold tongue is well developed and SST cooler than 25°C extends westward to 130°W. Temperature changes of 3°–4°C occur across the equatorial front. During El Niño years, SST in the cold tongue is elevated throughout the year; the equatorial front almost disappears.

Surface winds vary in concert with the changes in the SST distribution. The mean southeasterly winds are strongest during the cold season. As this southerly flow crosses the equatorial front it accelerates, leading to a pronounced horizontal divergence. During the cold season of the colder (i.e., non–El Niño) years, when the equatorial cold tongue and the oceanic front are most developed, the southerly surface wind on the equator is anomalously weak, but northward flow near 5°N is anomalously strong, and hence the divergence over the front is enhanced relative to the climatological mean.

Wallace et al. (1989) interpret these results as evidence that at least two processes are important in the dynamics of the surface wind field near the equator. The seasonal and interannual variability of surface wind is due, in part, to hydrostatic sea-level pressure changes induced by changes in the strength of the associated cold tongue. Such a direct coupling between

* Contribution Number 1051 from NOAA/Pacific Marine Environmental Laboratory.

*Corresponding author address:* Dr. Stanley P. Hayes, Pacific Marine Environmental Laboratory/NOAA, NOAA Building Number 3, 7600 Sand Point Way NE, Seattle, Washington 98115.

SST and sea-level pressure anomalies was discussed by Lindzen and Nigam (1987). However, Wallace et al. (1989) note that the sea-level pressure and the surface wind speed are not linearly related to each other or to the underlying SST gradient. They suggest that atmospheric boundary layer dynamics are responsible for this discrepancy. As boundary layer flow passes from the cold tongue to the warmer waters north of the equatorial front, the vertical stratification decreases. The wind shear near the sea surface is reduced and hence, surface wind speeds increase.

Wallace et al. (1989) confined their analyses to the seasonal and interannual variability. However, SST in the eastern Pacific also exhibits pronounced fluctuations on shorter time scales associated with upwelling events (Leetmaa and Wilson 1985) and tropical instability waves (Legeckis 1977; Philander 1978). The historical ship data are too sparse to resolve these higher frequency variations. However, relatively dense temporal and spatial resolution of the surface wind and SST fields at a few locations in the tropical Pacific Ocean are now being provided by moored buoy measurements made as a part of the Tropical Ocean–Global Atmosphere (TOGA) and Equatorial Pacific Ocean Climate Studies (EPOCS) programs. We report here analysis of the EPOCS (Hayes et al. 1986) measurements along 110°W between 5°N and 5°S (Fig. 1). Time series of daily averaged values obtained from November 1987 through December 1988 are considered. Meteorological instrumentation used on these buoys is discussed in Reynolds et al. (1989).

## 2. Tropical instability waves

Characteristics of tropical instability waves in the eastern Pacific have recently been reviewed by Legeckis (1986) and Halpern et al. (1988). The latter study used equatorial moored current measurements at several locations from 95° to 152°W to examine the spectral properties of the upper ocean meridional velocity. At periods near 20 days a statistically significant peak in meridional kinetic energy is observed at sites from 100° to 140°W. The zonal wavelength was estimated to be about 1300–1600 km and the westward phase speed about 80–90 cm s$^{-1}$. The oscillations are nonstationary and have maximum amplitude when the equatorial cold tongue and the associated equatorial front are well developed. The study found no evidence that the 20-day period waves were directly forced by the local surface wind.

The meridional surface velocity field discussed by Halpern et al. (1988) advects the background SST field and leads to undulations of the equatorial front (Pullen et al. 1987). These SST fluctuations are easily observed in time series of near equatorial temperature. In Fig. 2, wind vectors and SST contours constructed from the measurements at the five sites along 110°W during the period November 1987 through April 1988 are shown. The cusplike structures in SST near 2°N are evidence of the passage of tropical instability waves. The period between these cold events is approximately 30 days. They are quite pronounced from November through January, disappear briefly in February–March when the cold tongue vanishes, and reappear in March–April. At 2°N peak-to-trough temperature differences are 2°–3°C, and the temperature increase from the equator to 2°N ranges from 0°C to more than 3°C.

It is conceivable that these SST perturbations could induce boundary layer wind fluctuations similar to those described by Wallace et al. (1989). The undulations in the equatorial front associated with the waves should be reflected in the horizontal gradients of at-

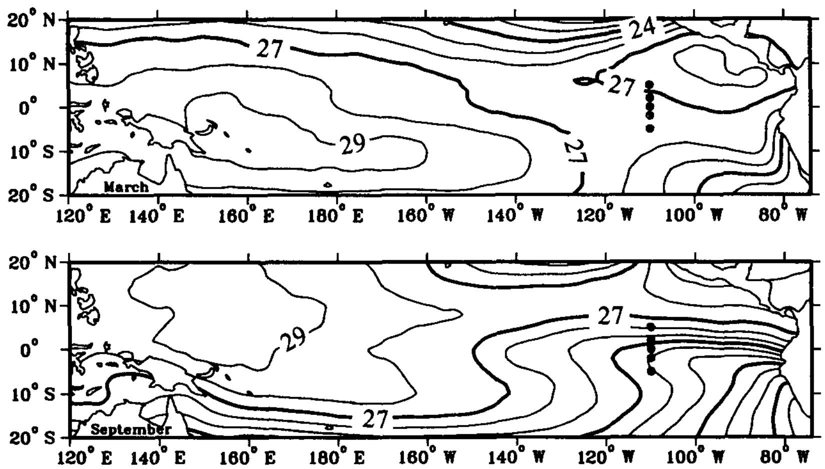


FIG. 1. Locations (dots) of the moored measurements of surface wind and SST superimposed on the climatological mean SST fields (Reynolds 1988) for March and September. Contour interval is 1°C.

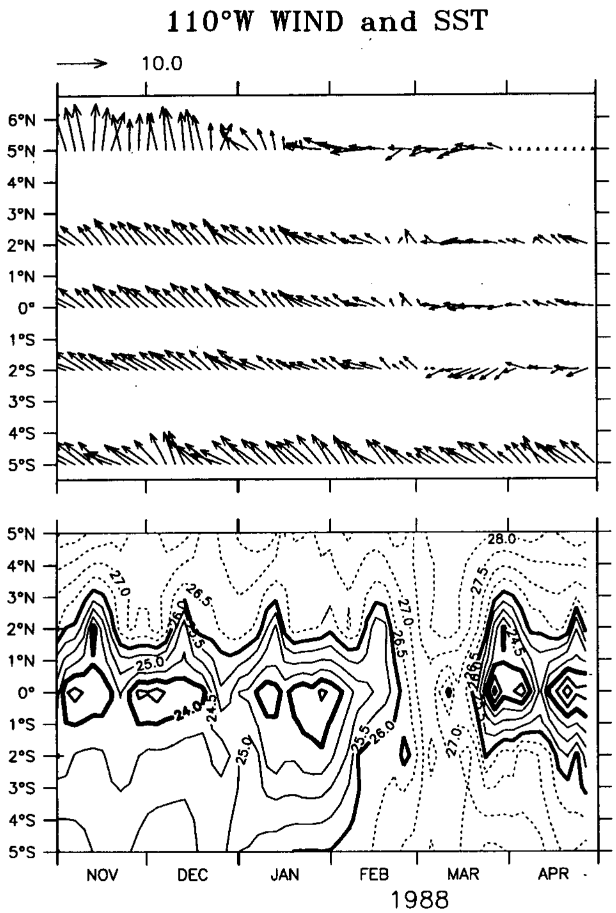


FIG. 2. Wind vectors and SST contours along 110°W based on the moored measurements at 5°N, 2°N, 0°, 2°S, and 5°S from November 1987 through April 1988. Time series were filtered with a 5-day Hanning filter prior to plotting. Wind and SST measurements at 5°N stopped on 30 March; after that time 20 m temperature was used in place of SST in the contour plot. Temperature contour interval is 0.5°C. Arrow at top of figure indicates scale of wind vectors in meters per second.

mospheric sea-level pressure and boundary layer stratification, either of which might influence the surface winds. These two processes are illustrated in Fig. 3 [note that the zonal (~1000 km) and meridional (~250 km) scales of the equatorial front perturbations have been distorted to make the figure more legible]. In the top panel, sea-level pressure is assumed to be high over the cold water and low over the warm water. Near the equator (ignoring Coriolis effects), boundary layer winds tend to be directed down the surface pressure gradient. As noted in the schematic, as the SST perturbations propagate westward, zonal winds and SST will be 90° out of phase; meridional winds will be either in phase or 180° out of phase with SST, depending upon the latitude relative to the equatorial front. On the other hand, if modification of boundary layer stratification by the SST field is the dominant process (bottom panel), then one should expect the prevailing southeasterly winds to be enhanced where the front is advected southward of its mean position by the waves and vice versa. In this case, warm SST anomalies will be associated with southeasterly wind anomalies.

Large-scale correlations of the wind and SST fields are obvious in Fig. 2. In November and December the southeast trade winds extend across the equator to beyond 5°N, becoming more southerly at the northern limit. SST is lowest in the equatorial cold tongue, but the entire belt from 5°N to 5°S is cool. In January the southerly winds begin to relax and by the end of the month the wind at 5°N is nearly easterly. During February this relaxation of the southeast trade winds moves southward across the array at least as far as 2°S. By the end of the month warm water (SST > 27°C) extends all across the array and there is no equatorial cold tongue. In March and April equatorial winds become predominantly easterly and strengthen. The equatorial cold water returns; however, it is confined to within 2° of the equator. The SST difference between 5°N and 5°S is small (<0.5°C) compared to what it had been during the previous cold period. Near the equator winds over the cold tongue are meridionally divergent.

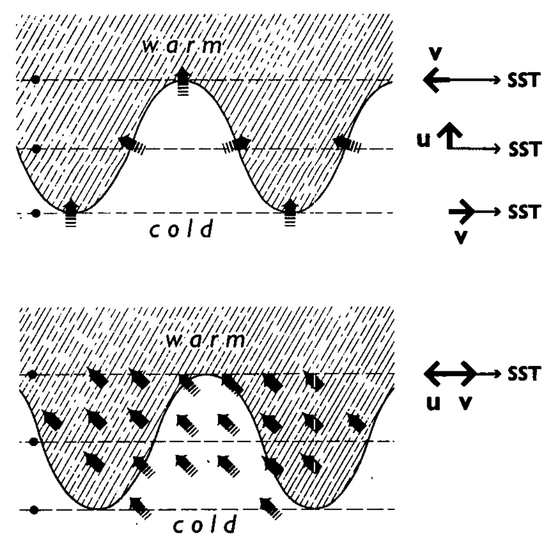


FIG. 3. Schematic representation of the expected perturbation of the surface wind field caused by a westward propagating SST field associated with a tropical instability wave in the eastern equatorial Pacific. Top panel assumes principal forcing is through the hydrostatic influence on the atmospheric sea-level pressure (SLP) as discussed in Lindzen and Nigam (1987). Warm SST is associated with low SLP, cool water with high SLP. Near the equator surface winds tend to flow down the SLP gradient. As summarized by the diagram on the right, zonal wind ($U$) perturbations are 90° out of phase with the SST while meridional wind changes tend to be either in phase or 180° out of phase depending upon the latitude. Bottom panel assumes that the principal coupling of SST and wind is through modification of boundary layer shear as discussed in Wallace et al. (1989). In this case surface winds are stronger over warm SST. For the southeasterly winds shown, zonal winds are 180° out of phase with SST perturbations and meridional winds are in phase with them.

Largest SST perturbations were observed in the equatorial cold tongue between 2°N and 2°S. To investigate the changes in the surface winds as they crossed this region of varying SST, we examined the correlations between SST and wind and between their meridional gradients. Meridional gradients are sensitive to small-scale fluctuations that might be associated with the local SST distribution, as opposed to the wind field itself, which may exhibit substantial variability at these frequencies in association with atmospheric, planetary-scale disturbances unrelated to local air–sea interaction. The strongest and most consistent correlations are associated with the meridional gradients, as discussed below.

In Fig. 4, time series for the wind components at 2°N, 2°S, and the equator are shown. All series have been low-pass filtered with a 5-day full-width Hanning filter. The top panel shows the average for the three latitudes, and the other panels show the meridional gradients of SST and meridional wind. The mean wind

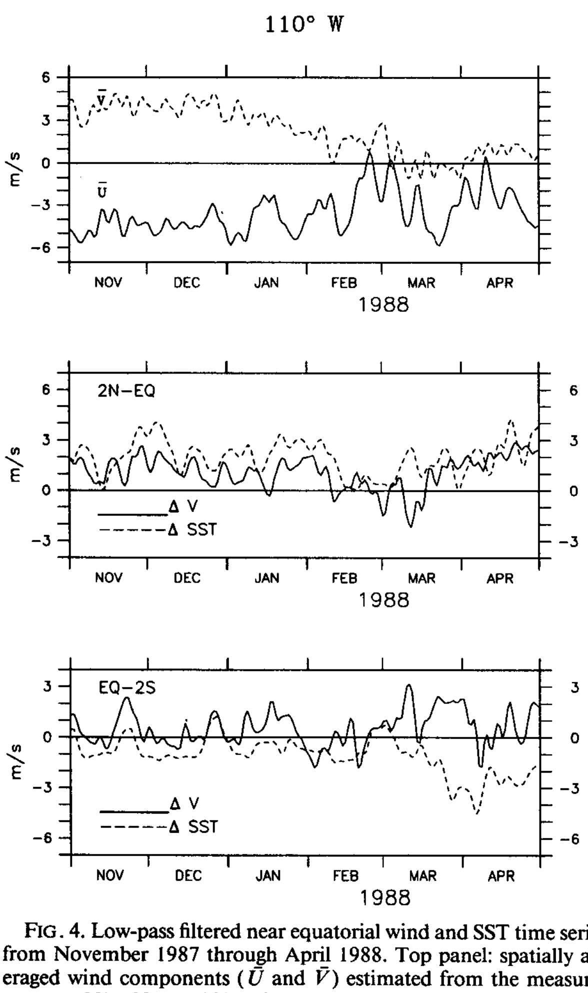


FIG. 4. Low-pass filtered near equatorial wind and SST time series from November 1987 through April 1988. Top panel: spatially averaged wind components ($\bar{U}$ and $\bar{V}$) estimated from the measurements at 2°N, 0°, and 2°S. Middle panel: the difference in meridional wind and SST between 2°N and the equator. Bottom panel: the difference in meridional wind and SST between the equator and 2°S.

near the equator is southeasterly from November through January. The southerly component decreases during February and remains weak for the rest of the record. Easterly winds also drop off during February, but return quite strong for a few weeks in late March and again during April. The period with the most nearly constant wind is the first three months of the record.

The gradients in meridional wind and SST between 2°N and the equator are clearly correlated. When the temperature at 2°N is high relative to the equator, then the meridional wind is stronger at 2°N. During the first half of the record, correlated fluctuations on a variety of time scales appear in the wind and SST gradient. For these three months the correlation coefficient ($R$) is 0.60, which is significant with 95% confidence [significance levels are based on the number of degrees of freedom that are estimated from the integral time scales of the series (Davis 1976)]. In the second half of the record, the predominant signal in both SST and wind gradient is a trend towards increasing SST and meridional wind at 2°N relative to 0°. Maximum wind divergence in April is about $10^{-5}$ $s^{-1}$, associated with a temperature gradient of about 1.3°C per degree of latitude. Over the complete six-month record the correlation between SST gradient and meridional wind gradient is 0.51 (significant at the 95% level). For both the six-month and three-month periods the maximum correlation occurs at zero lag. Note that the shortest resolvable lag between the 5-day Hanning low-pass filtered series is 1.25 days. All correlations reported here are the maxima of the cross-correlation function and occur at zero lag within this limit of resolution.

SST gradients between the equator and 2°S are relatively small (about 1°C) for the first half of the record; the equator is generally colder than 2°S. Meridional wind and SST gradients during this period are correlated. For example, in late November and again in late December warm surface water moved southward onto the equator, apparently in association with the instability wave activity. At these times SST is higher and northward wind speed is stronger on the equator than at 2°S. For the three months from November to January the correlation is significant ($R$ = 0.63). During the latter half of the record, when the mean meridional wind was weak, the correlations are much smaller.

The seasonal change in winds and SST from November–January to February–April complicates the interpretation of the data in Figs. 2 and 4. More uniform conditions are observed during the second six-month interval considered: July through December 1988. During this period, the spatially averaged near-equatorial winds are consistently from the southeast (Fig. 5, top panel). The equatorial cold tongue is anomalously strong [the six-month mean equatorial SST is 20.4°C compared to a climatological mean value of 23.5°C (Reynolds 1988)] and the equatorial front is well developed. The signature of the tropical instability waves is clearly apparent in satellite derived SST

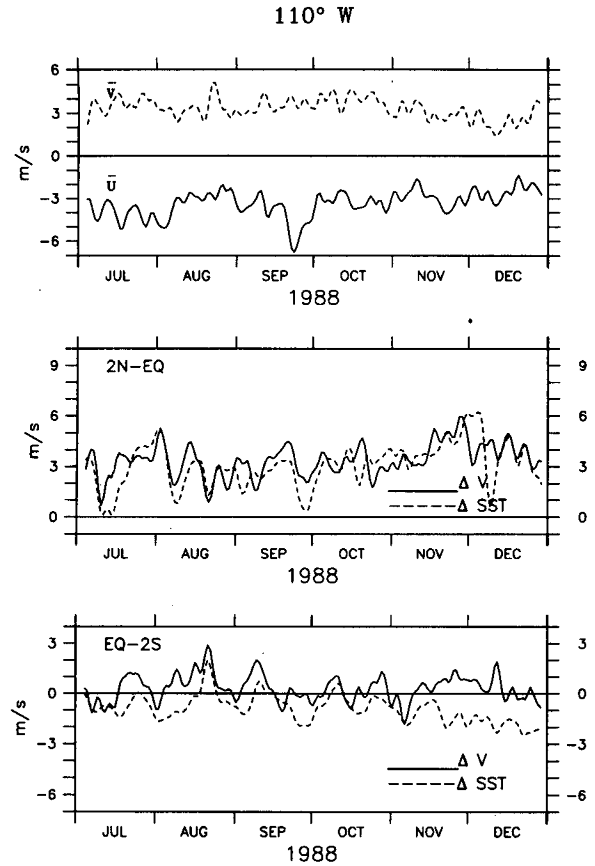


FIG. 5. As in Fig. 4 for the period July 1988 through December 1988.

fields (Legeckis, personal communication) and the buoy record at 2°N.

Correlations between the meridional gradient of SST and the meridional wind component are again positive (Fig. 5, lower panels). Because wind direction was reasonably constant, correlation coefficients between wind and SST could be computed over the entire six-month record. Both north and south of the equator, the meridional wind and SST gradients are significantly correlated ($R = 0.6$). Between 2°N and the equator there is a mean meridional wind divergence of nearly 1.5 $\times 10^{-5}$ s$^{-1}$ and a mean temperature gradient of about 1°C per degree of latitude. South of the equator the mean divergence is near zero. However, the cross-equatorial excursion of the equatorial front in late August, during which the equator was about 2°C warmer than 2°S, is accompanied by a wind divergence of 1.3 $\times 10^{-5}$ s$^{-1}$.

During this six-month interval of persistent southeast trade winds, zonal wind fluctuations are also correlated with SST changes (Fig. 6, upper panel). Higher correlation coefficients are again obtained when meridional gradients of wind and SST are considered. Significant (with 95% confidence) correlations are found between zonal wind and SST gradient between 2°N and the equator ($R = -0.66$) and between the equator and 2°S ($R = -0.73$). Because the winds are always blowing from the southeast, the sign of the correlation coefficient indicates that wind speeds tend to be stronger over warm water.

The phase relationships in Figs. 4–6 indicate that boundary layer stability is the key factor in the atmospheric response to the SST fluctuations associated with instability waves. Indeed, the strongest correlation observed is between meridional gradients of wind speed and SST (Fig. 6, lower panels). North of the equator (2°N–0°) the correlation coefficient is 0.75, and south of the equator (0°–2°S) it is 0.83. It is evident from the figure that the fluctuations in wind speed associated with the passage of the instability waves are as large as 1–2 m s$^{-1}$.

## 3. Discussion and conclusions

Analysis of moored array measurements of SST and surface wind in the eastern equatorial Pacific shows

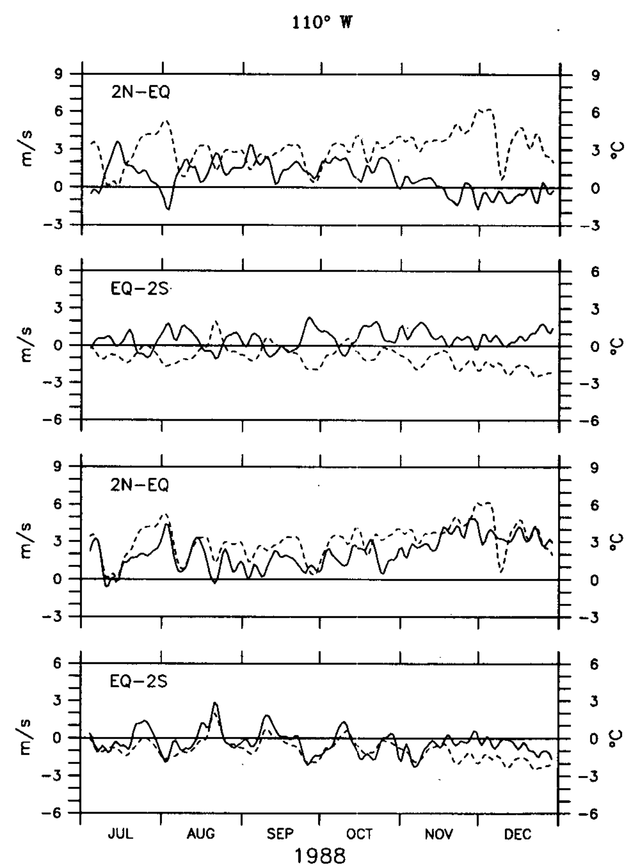


FIG. 6. Low-pass filtered time series during the period July through December 1988. Top two panels are the differences in zonal wind (solid) and SST (dashed) between 2°N and the equator and between the equator and 2°S; bottom two panels are the differences in scalar wind speed (solid) and SST (dashed) over the same latitudes.

evidence of wind fluctuations that are driven by local perturbations in SST associated with the tropical instability waves with periods near 20 days and a meridional scale of a few degrees of latitude. Two six-month records from locations that spanned the equatorial cold tongue (2°N, 0°, and 2°S along 110°W) were examined. During periods when the southeast trade winds were strong (November 1987 through January 1988 and, particularly, July 1988 through December 1988), the correlations between wind and SST gradients are pronounced. In the latter period, meridional gradients of the wind components and the wind speed are all correlated with SST gradients. The phase relationships indicate that southeasterly trades tend to be enhanced during periods of warm SST and vice versa, so that the band of strong divergence in meridional wind remains over the equatorial front as it meanders northward and southward. Wallace et al. (1989) also found a close correspondence between the divergence of the meridional component of surface wind and the SST front on annual and interannual time scales.

In their study of the tropical instability waves in the ocean, Halpern et al. (1988) found enhanced meridional wind variance in the period band centered on the instability wave maximum energy (0.05 cpd), but no significant coherence between local surface wind components and ocean currents. This result appears to conflict with the correlations reported here; however, in the present study significant correlations were only obtained when meridional differences in surface winds were compared to SST. Using differences in place of the winds themselves removes some of the large-scale wind variations and permits examination of local effects.

In studies of atmosphere–ocean interactions based on observed correlations, it is often difficult to distinguish between cause and effect. However, in the present case one can be quite confident that the correlations are a reflection of the atmospheric response to the ocean. For example, the correlations indicate that, relative to 2°S, wind speed and SST fluctuations on the equator are in phase. This relation would not be expected if the ocean were responding to the wind perturbations, because enhanced southeasterlies at the equator would produce cooler SST by a combination of upwelling, advection of colder water from the east, and increased evaporation.

The positive correlation between wind speed and SST supports the hypothesis that in the eastern equatorial Pacific, modification of the boundary layer shear rather than changes in the atmospheric sea-level pressure gradient is the dominant process affecting surface winds on the time scales studied. As discussed by Wallace et al. (1989), surface winds can vary substantially in response to changes in the stratification of the planetary boundary layer, even in the presence of a uniform wind field a few hundred meters above the surface. An unstable stratification that occurs when cold air passes over warmer water favors stronger surface winds and vice versa. This relation suggests that surface wind speed should be negatively correlated with air–sea temperature difference. This correlation was examined at each buoy site for the July–December 1988 period. In this case, to isolate the smaller spatial scale wind fluctuations, the spatially averaged (average of 2°N, 0°, and 2°S) wind speed time series was removed from the time series of speed at each site before the correlations with the air–sea temperature difference were computed. Significant correlations (with 95% confidence) are found at all sites: $R$ (2°N) = −0.50; $R$ (0°) = −0.66; $R$ (2°S) = −0.76.

It is interesting that the correlations between wind speed and SST gradient (Fig. 6) or air–sea temperature difference are somewhat stronger south of the equator even though the SST perturbations are generally larger north of the equator. The vertical wind shear in the surface layer should be strongest and it may well be most sensitive to the underlying SST in the region of the cold tongue, where the stratification is strongest.

The strong climatological mean SST gradients and the modulation of these gradients by the tropical instability waves make the eastern equatorial Pacific an interesting region for the study of local air–sea interactions. Week-to-week SST perturbations associated with the instability waves are a convenient probe with which to examine the atmospheric response. These waves are most pronounced during the cold SST season when the southeast trade winds are reasonably constant (Legeckis 1986; Halpern et al. 1988); hence, interpretation of the atmospheric signal is simplified. The strong correlations between SST and surface wind speed that we have observed indicate a rapid and direct atmospheric response to the SST perturbations. Estimates of net surface heat flux into the ocean also indicate the importance of the instability wave SST fluctuations (Imawaki et al. 1988). Additional buoy measurements (e.g., atmospheric pressure, solar radiation, and humidity) and vertical profiles of the atmospheric boundary layer are required in order to better understand the processes that lead to this coupling.

*Acknowledgments.* The assistance of H. P. Freitag, L. Gearin, L. Mangum, and N. N. Soreide in this analysis is gratefully acknowledged. C. Deser provided helpful comments on a draft version of the manuscript. This work was supported, in part, by the Equatorial Pacific Ocean Climate Studies (EPOCS) Project of NOAA/ERL (SPH, MJM) and by the Climate Dynamics Program of the National Science Foundation under Grant ATM-8318853 (JMW).

## REFERENCES

Davis, R. E., 1976. Predictability of sea surface temperature and sea level pressure anomalies over the North Pacific Ocean. *J. Phys. Oceanogr.*, **6**, 249–266.

Halpern, D., R. A. Knox and D. S. Luther, 1988. Observations of

20–day period meridional current oscillations in the upper ocean along the Pacific equator. *J. Phys. Oceanogr.*, **18**, 1514–1534.

Hayes, S. P., D. W. Behringer, M. Blackmon, D. V. Hansen, N.-C. Lau, A. Leetmaa, S. G. H. Philander, E. J. Pitcher, C. S. Ramage, E. M. Rasmusson, E. S. Sarachik and B. A. Taft, 1986. The Equatorial Pacific Ocean Climate Studies (EPOCS) Plan: 1986–1988. *Eos, Trans. Amer. Geophys. Union,* **67,** 442–444.

Imawaki, S., P. P. Niiler, C. H. Gautier, D. Halpern, R. A. Knox, W. G. Large, D. S. Luther, J. C. McWilliams, J. N. Moum and C. A. Paulson, 1988. A new method for estimating the turbulent heat flux at the bottom of the daily mixed layer. *J. Geophys. Res.,* **93,** 14 005–14 014.

Leetmaa, A., and D. Wilson, 1985. Characteristics of near-surface circulation patterns in the eastern equatorial Pacific. *Progress in Oceanography,* Vol. 14, Pergamon, 339–352.

Legeckis, R., 1977. Long waves in the eastern equatorial Pacific Ocean: A view from a geostationary satellite. *Science,* **197,** 1179–1181.

——, 1986: A satellite time series of sea-surface temperatures in the eastern equatorial Pacific Ocean. *J. Geophys. Res.,* **91,** 12 879–12 886.

Lindzen, R. S., and S. Nigam, 1987. On the role of sea-surface temperature gradients in forcing low-level winds and convergence in the tropics. *J. Atmos. Sci.,* **44,** 2440–2458.

Philander, S. G. H., 1978. Instabilities of zonal equatorial currents 2. *J. Geophys. Res.,* **83,** 3679–3682.

Pullen, P. E., R. L. Bernstein and D. Halpern, 1987. Equatorial long-wave characteristics determined from satellite sea surface temperature and in situ data. *J. Geophys. Res.,* **92,** 742–748.

Reynolds, R. W., 1988. A real-time global sea surface temperature analysis. *J. Climate,* **1,** 75–86.

——, K. Arpe, C. Gordon, S. P. Hayes, A. Leetmaa and M. J. McPhaden, 1989. A comparison of tropical Pacific surface wind analyses. *J. Climate,* **2,** 105–111.

Wallace, J. M., T. P. Mitchell and C. Deser, 1989. The influence of sea surface temperature on surface wind in the eastern equatorial Pacific: Seasonal and interannual variability. *J. Climate,* **2,** 1492–1499.